Bull. Mater. Sci. (2021) 44:37
https://doi.org/10.1007/s12034-020-02342-w

Structural, elastic and mechanical properties of Ti–15Nb–*x*Ge alloys: insight from DFT calculations

E GÜLER[1,*], G UĞUR[2], Ş UĞUR[2], M GÜLER[1] and R KHENATA[3]

[1]Department of Physics, Ankara Hacı Bayram Veli University, 06900 Ankara, Turkey
[2]Department of Physics, Gazi University, 06500 Ankara, Turkey
[3]Laboratoire de Physique Quantique et de la Matière et de Modélisation Mathématique (LPQ3M), Université de Mascara, 29000 Mascara, Algeria
*Author for correspondence (eguler71@gmail.com)

MS received 7 July 2020; accepted 15 September 2020

Abstract. We theoretically investigated the structural, elastic and mechanical properties of Ti–15Nb–*x*Ge alloys with $x = 0.8$, 1, 1.2, 1.4, 1.6 and 1.8 (wt%) compositions for the first time. Theoretical calculations were performed with the generalized gradient approximation (GGA) functional within density functional theory (DFT). We employed the Perdew–Burke–Ernzerhof (PBE) scheme and the virtual crystal approximation (VCA) in this study. We determined the elastic constants, bulk, shear and Young's moduli, Pugh ratio, Poisson's ratio, universal anisotropy and hardness of all the alloys under varying Ge% concentrations. All studied compositions of the alloys show structural stability. Young's moduli values were obtained as 43 and 14.8 GPa for Ti–15Nb–0.8Ge and Ti–15Nb–1.8Ge alloys, respectively, which compare well to the Young's moduli range of human cortical bone with 10–30 GPa. Except the Poisson's and Pugh ratios, all other computed parameters of the alloys were found to decrease under increasing Ge concentrations. Further, all investigated alloys exhibit desired ductile mechanical behaviour of biomaterials and calculated hardness values of these alloys are satisfactory with the hardness of human teeth dentin.

Keywords. Ti–Nb; Ti–Nb–Ge; biomaterials; elastic properties; mechanical properties; DFT.

1. Introduction

It is well accepted in the biomaterials' community that metallic alloys used in biomedical applications for human implants should have good corrosion resistance, good ductility, low elastic modulus, non-toxic and non-allergic abilities [1–5]. On the other hand, in particular, for the bone implants, invention of new materials that meet all the above standards for biomedical applications with a modulus near the human cortical bone (10–30 GPa) has always been a major challenge for scientists [6–11]. Biomaterials with a higher elastic modulus than human bones lead to a flexible mismatch between the implant, which results in resorption of bones after implantation. This case is also known as stress shielding which may also lead to contact loosening, implant failure or debris-induced infections in the human body [2,12–15]. To overcome these challenges, researches have been extensively focussed on the existing difficulties and aimed to develop new materials for practical applications as biomaterials. At this point, the use of Ti alloys is of importance due to their good mechanical and corrosion properties as well as excellent biocompatibility [16–20]. Exemplarily, for orthopaedic implants, one of the most desired mechanical feature is the stiffness which is directly proportional to elasticity modulus or so-called Young's modulus (E). A Young's modulus value analogous to that of the bone will afford the necessary 'isoelastic behaviour' between implanted material and bone. However, the most generic Ti-based alloys applied in orthopaedics display relatively high elastic modulus values ($\sim$110–120) GPa compared with those of the human cortical bone (10–30 GPa). Therefore, much effort is currently dedicated to the improvement of new binary, ternary and multicomponent titanium alloys with reduced elastic modulus [21–23]. Amongst them, Ti–Nb binary, ternary and multicomponent alloys and their derivatives become more prominent because of their low elastic modulus (i.e., Ti–40Nb with 65 GPa), shape memory effect and super elasticity [24]. Further, the elements, such as Sn, Ta, Pd, Zr, Mo and Cu are added to broaden the composition range of binary Ti–Nb alloys which can improve the mechanical properties of the Nb alloys and are harmless to the human body [25]. There are several theoretical and experimental attempts carried out for ternary Ti–Nb–X [26–31] and for multicomponent Ti–Nb alloys [32,33] and so forth, in which most of their motivation is, obtaining a low Young's modulus compatible with the different parts of the human body. Some other examples that we came across for ternary Ti–Nb–X biomaterials for X alloying element are given with Cr in ref. [7], with Zr in refs.

Published online: 15 February 2021

[8,20], with In in ref. [10], with Sn in refs. [12,25], with Mo in ref. [23], with Si in ref. [28], with Al in ref. [33] as a third or fourth alloying component.

Even though the element Ge has an attractive potential for dental applications with no toxicity, good mechanical performance, corrosion resistant and processability [3], little is known about the addition of the Ge element as a third or further alloying element to one of the most important biomaterial groups of the Ti–Nb–X alloys. So, this existing shortness inspired us to do this theoretical study for Ti–15Nb–*x*Ge alloys with x = 0.8, 1, 1.2, 1.4, 1.6 and 1.8 compositions for the first time.

The next part of the paper provides our computational procedure where the results and discussion part of the work is presented in section 3 and conclusions of the study in section 4.

2. Computational details

We performed all the calculations with CASTEP code [34,35] in this research which allows the self-consistent DFT calculations within a plane-wave pseudopotential approach. During our calculations, we applied Perdew–Burke–Ernzerhof (PBE) exchange–correlation parameterization of the generalized gradient approximation (GGA) functional in the terms of electron–electron interactions for geometry optimization of the surveyed materials [36,37]. Further, the ion and electron interactions were carried out by employing the ultra-soft Vanderbilt pseudopotential scheme [38] and the electronic wave functions were treated as plane waves with 520 eV cut-off energy. For Brillouin zone sampling, we applied 10 × 10 × 6 Monkhorst–Pack grids [39]. The electronic valence configurations for the components of Ti–15Nb–*x*Ge alloys were $3s^2\ 3p^6\ 3d^2\ 4s^2$ for Ti element, $4s^2\ 4p^6\ 4d^4\ 5s^1$ for Nb element and $3d^{10}\ 4s^2\ 4p^2$ for Ge element, respectively, through the virtual crystal approximation (VCA) method [40]. VCA method is much simpler and computationally less-expensive approach with regard to the commonly used supercell method of crystal structures. As well, it allows the investigations of mixed-type crystals by conserving the unit cell of the initial material [40]. After checking the crystal structure of α-phase of pure Ti, we then designed the Ti–15Nb alloy and switched to the other alloys by adding small Ge concentrations changing from x = 0.8–1.8 in steps of 0.2 Ge (wt%) and completed our calculations.

3. Results and discussion

3.1 *Elastic stiffness constants and structural stability of Ti–15Nb–xGe alloys*

As declared often in the published literature [1–33], Ti is a multiphase crystalline metal with a hexagonal close packed (α-phase) structure at room temperature and can transform into a body centred cubic (β phase) structure at temperatures above the 882°C [1]. Besides, the β phase of the Nb alloys begins to occur with the addition of at least 35–40% Nb to α-Ti. However, as emphasized in ref. [1], since Nb is a rare metal with a high melting point, using less Nb element during alloying with Ti is really beneficial for low-cost manufacturing and other production perspectives. Therefore, after deciding to keep Nb composition at 15% (α-phase), we performed further runs for Ti–15%Nb, thanks to VCA as told. Thus, we were able to check and compare our results with prior experimental and theoretical data of the elastic and mechanical properties of α-Ti and Ti–15%Nb.

For hexagonal crystals, five independent elastic constants exist, namely, C_{11}, C_{12}, C_{13}, C_{33} and C_{44}. These elastic constants are not only responsible for mechanical hardness, but also necessary to identify the stability of a given material [41]. Although elastic constants usually derived from the total energy calculations represent the single-crystal elastic properties, Voigt–Reuss–Hill approach is a reliable scheme for elastic constants of polycrystalline materials [41]. To hold the right values of elastic constants and associated parameters of α-Ti, we took into account the Voigt–Reuss–Hill values during calculations. Figure 1 shows five typical elastic constants of pure titanium (α-phase) along with the former theoretical studies of refs. [29,42] and the experimental data [43] with their values listed in table 1. Our present computed values for the elastic constants of α-phase of Ti correspond well to former results [29,42,43] as seen in figure 1 and table 1. Moreover, from the stability outlook, these elastic constants (C_{11}, C_{12}, C_{13}, C_{33} and C_{44}) must satisfy the conventional Born mechanical stability requirements of hexagonal crystals expressed as follows:

$$C_{44} > 0, C_{11} > C_{12} \text{ and } (C_{11} + 2C_{12})C_{33} - 2C_{13}^2 > 0.$$

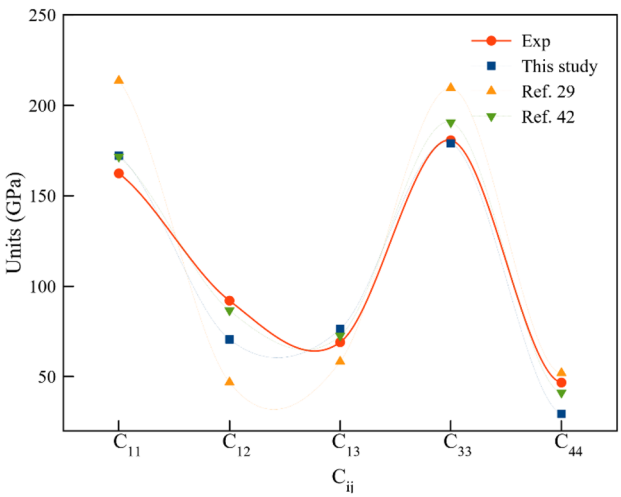

Figure 1. Elastic stiffness constants of α-Ti.

Table 1. A comparison for the elastic stiffness constants of α-Ti, Ti–15Nb and Ti–15Nb–*x*Ge alloys.

Alloy	C_{11} (GPa)	C_{12} (GPa)	C_{13} (GPa)	C_{33} (GPa)	C_{44} (GPa)
α-Ti (this work)	172.2	70.6	76.3	179.0	29.4
Ref. [29]	213.7	46.8	58.3	209.6	52.0
Ref. [42]	171.6	86.6	72.6	190.6	41.1
Exp. [43]	162.4	92.0	69.0	180.7	46.7
Ti–15Nb (this work)	172.5	82.2	79.1	180.6	20.5
Ti–15Nb (Ref. [29])	197.9	65.5	61.2	223.8	30.5
Ti–15Nb–0.8Ge	128.7	78.9	71.6	139.0	6.0
Ti–15Nb–1Ge	126.2	81.6	75.2	137.8	4.4
Ti–15Nb–1.2Ge	114.0	75.1	69.3	126.6	3.2
Ti–15Nb–1.4Ge	107.5	73.5	67.0	119.5	2.1
Ti–15Nb–1.6Ge	100.8	71.3	65.4	113.5	1.2
Ti–15Nb–1.8Ge	93.6	68.4	62.6	114.5	0.1

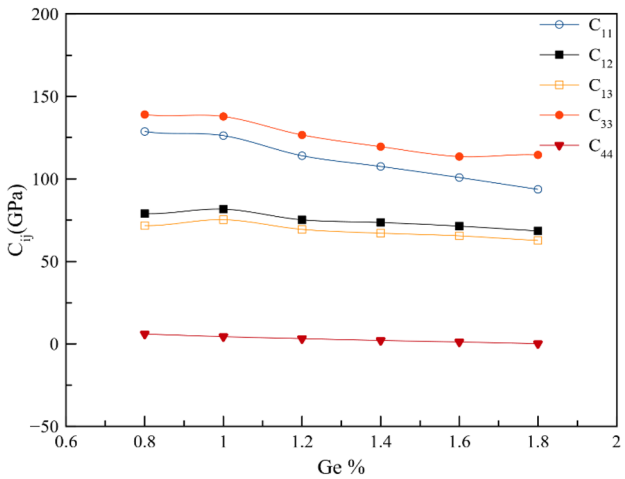

Figure 2. Elastic stiffness constants of Ti–15Nb–*x*Ge alloys.

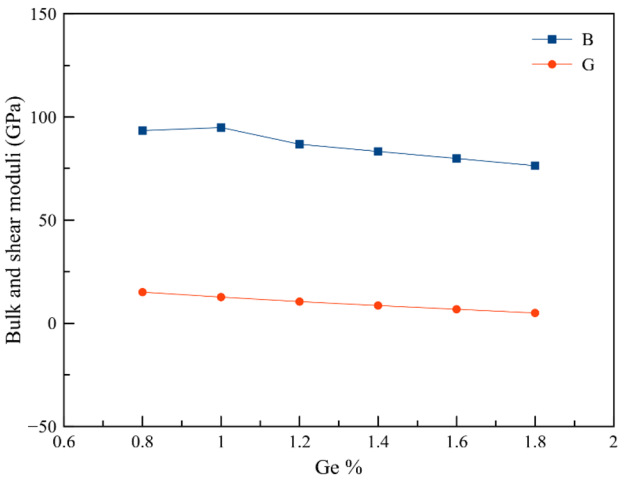

Figure 3. Bulk (*B*) and shear (*G*) moduli of Ti–15Nb–*x*Ge alloys.

Thus, as can be seen from figure 1 and table 1, the results for the elastic constants of α-Ti fulfill the Born mechanical stability rules and in the order of $C_{33} > C_{11} > C_{12} > C_{13} > C_{44}$ consistent with the earlier findings of refs. [29,42,43]. We should also mention here that similar trends are valid for the elastic constants of Ti–15%Nb alloy listed in table 1. Except the elastic constant C_{44}, all other stiffness constants of α-Ti show slight increments after the addition of 15%Nb. In figure 2, a clear decrement on the elastic constants begins to appear with the Ti–15%Nb–0.8Ge alloy. The other related studies with different compositions of Ge (1–1.8%) also mimic this behaviour. In other words, adding Ge element to the Ti–15%Nb alloy clearly reduce the elastic stiffness constants of these alloys keeping Born stability conditions and magnitude order of elastic constants in the range of $C_{33} > C_{11} > C_{13} > C_{12} > C_{44}$. As a result, obtained values for present calculated elastic stiffness constants and presence of mechanical stability character of considered alloys are in the range of formerly reported works of Ti–Nb alloys [29] as also seen in table 1.

3.2 *Elastic moduli of Ti–15Nb–xGe alloys*

Figure 3 shows two different elastic moduli namely bulk modulus (*B*) and shear modulus (*G*) of Ti–15Nb–*x*Ge alloys for the surveyed Ge range. Bulk modulus is a distinctive mechanical property that gives enough information about the bonding strength for materials. Also, it can be specified as the resistance of a given material to external deformations [41,44–48] where the shear modulus outlines the resistance response of a material exposed to shearing force [41,44–48]. As obvious in figure 3, both bulk and shear moduli of Ti–15Nb–*x*Ge alloys reduce with increase in the Ge concentrations.

Young's modulus (*E*), defines the resistance of the materials under uniaxial tensions and indicates the materials

degree of stiffness i.e., the higher value of E, the stiffer is the material [41,44–48]. To further ensure our study, we first computed Young's modulus of Ti–15Nb alloy and compared with very recent experimental value of ref. [1]. Our computed value of the Young's modulus of Ti–15Nb alloy is 91.5 GPa that corresponds well the experimental value of 87.9 GPa [1] as listed in table 2. On the other hand, since low elastic modulus value is one of the key and desired features of an acceptable biomaterial, we plotted the Young's modulus of Ti–15Nb–xGe alloys *vs.* changing Ge concentrations in figure 4. As obvious in figure 4, the highest Young's modulus of Ti–15Nb–xGe alloys arises at 43 GPa with 0.8% Ge and its lowest value appears at 14.8 GPa with 1.8% Ge addition. Thus, we can easily conclude that small additions of Ge element (1–2%) to Ti–15Nb alloys yield the most necessary biomaterial property with low elastic modulus since being in the order of human cortical bone elastic modulus (10 and 30 GPa). In other words, Ti–15Nb–xGe alloys can be novel and strong candidate of biomaterial science and technology, in particular, for the practical applications and usage in human body. As another crucial point, one should remember that the increasing of Ge content in Ti–15Nb alloys causes the decrement of Young's modulus which tells us that the study can be further enhanced for other compositions of Ti–Nb alloys with Ge especially with higher elastic modulus values. In addition, a quick look at table 2 reveals all our computed values of B, G and E moduli are satisfied within the experimental and theoretical results of α-Ti and Ti–Nb alloys.

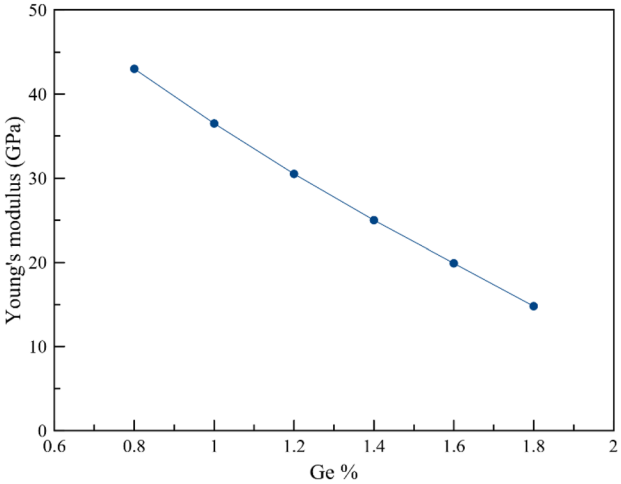

Figure 4. Young's modulus (E) of Ti–15Nb–xGe alloys.

3.3 *Ductility of Ti–15Nb–xGe alloys*

Since ductility and brittleness are two important mechanical properties for materials manufacturing, we also investigated the ductile (brittle) behaviour of Ti–15Nb–xGe alloys. Brittle and ductile adjectives signify the two discrete mechanical characters of solids when they are subjected to external deformations. For many brittle materials, external deformation does not much affect them and they behave less deformable before fracture. Oppositely, ductile materials show a much deformable nature before fracture [41,44–48]. For the separation of ductile and brittle materials from each other, Pugh's B/G ratio analysis is a reliable threshold. According to Pugh, if the B/G ratio of a material is about 1.75 and higher, the related material is considered to be ductile, otherwise as brittle [49]. Figure 5 shows the B/G ratios of Ti–15Nb–xGe alloys. Ti–15Nb–xGe alloys indicate an apparent ductility under different Ge concentrations. The ductility of these alloys increases by increase in the Ge content as in figure 5 which meets one of the most required features of biomaterials.

3.4 *Poisson's ratio of Ti–15Nb–xGe alloys*

As another mechanical property, Poisson's ratio (ν) represents the ratio between the transverse strain (e_t) and longitudinal strain (e_l) in the elastic loading direction of the

Table 2. Other mechanical parameters of α-Ti, Ti–15Nb and Ti–15Nb–xGe alloys.

Alloy	B (GPa)	G (GPa)	B/G	E (GPa)	ν	A_U	H_{Tian} (GPa)
α-Ti (this work)	107.7	40.5	2.65	108.2	0.332	0.352	4.175
Ref. [29]	108.7	67.4	1.61	167.3			
Ref. [42]	110.8	44.6	2.48	118.1			
Exp. [43]	107.3	43.4	2.47	114.6			
Ti–15Nb (this work)	111.8	33.5	3.33	91.5	0.363	0.86	2.810
Ti–15Nb (Ref. [29])	115.1	49.6	2.32	129.5			
Ti–15Nb–0.8Ge	93.4	15.1	6.18	43.0	0.423	3.42	0.794
Ti–15Nb–1Ge	94.9	12.7	7.47	36.5	0.435	4.75	0.556
Ti–15Nb–1.2Ge	86.8	10.5	8.26	30.5	0.441	6.03	0.446
Ti–15Nb–1.4Ge	83.3	8.6	9.68	25.0	0.449	8.85	0.322
Ti–15Nb–1.6Ge	79.9	6.8	11.75	19.9	0.458	15.02	0.220
Ti–15Nb–1.8Ge	76.4	5.0	15.28	14.8	0.467	131.6	0.132

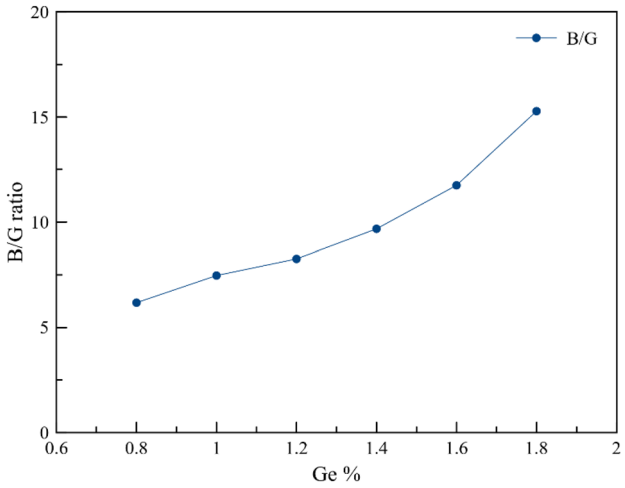

Figure 5. Ductile behaviour of Ti–15Nb–*x*Ge alloys.

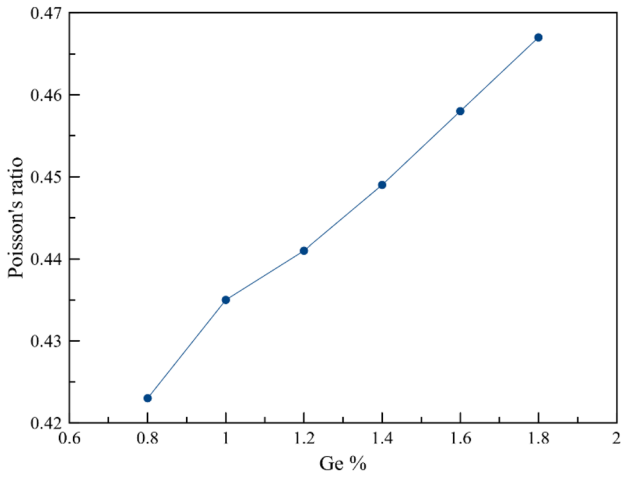

Figure 6. Poisson's ratio of Ti–15Nb–*x*Ge alloys.

regarding material. It also conveys valuable hints about the bonding force in solids [41,44–48]. The Poisson's ratio values with $v = 0.25$ and 0.5 indicate the lower and upper thresholds of the central forces of solids, respectively. In our study, the Poisson's ratio of Ti–15Nb–*x*Ge alloys takes place between 0.42 and 0.46 as in figure 6 being above the typical Poisson's ratio value of metals with 0.35. Our computed Poisson's ratio results suggest that the bonding forces in Ti–15Nb–*x*Ge alloys mainly originate from the central forces. As well, increasing Ge content in these alloys also raises the Poisson's ratio of Ti–15Nb–*x*Ge alloys as seen in figure 6.

3.5 *Elastic anisotropy of Ti–15Nb–xGe alloys*

The formation of microcracks in the materials is strongly associated with the elastic anisotropy [50]. Hence, we calculated the elastic anisotropy values of Ti–15Nb–*x*Ge alloys. Although many determination indices were proposed for the elastic anisotropy of materials, we checked our

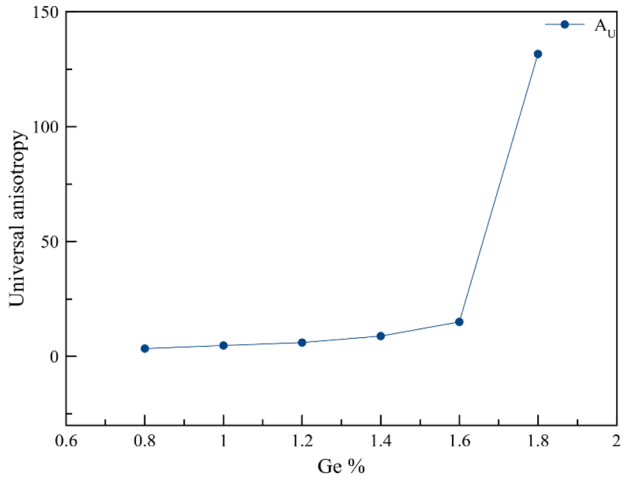

Figure 7. Universal anisotropy parameters of Ti–15Nb–*x*Ge alloys.

results with one of the most relevant indicators, namely, the universal elastic anisotropy (A_U) [50]. Universal elastic anisotropy can be expressed by the relation:

$$A_U = 5(G_V/G_R)/(B_V/B_R) - 6 \geq 0,$$

where the subscript V and R symbolize the Voigt and Reuss values of shear and bulk moduli of the associated material. For A_U values, any deviation from zero indicates the presence of elastic anisotropy. Figure 7 represents the elastic anisotropy behaviour of Ti–15Nb–*x*Ge alloys *vs.* increasing Ge concentrations. As seen in figure 7, elastic anisotropy values for Ti–15Nb–*x*Ge alloys starts with 3.42 and increase by the rising Ge content to a notable high value of 131.6 at 1.8% Ge concentration. So, we can state that Ti–15Nb–*x*Ge alloys are highly anisotropic even under small Ge additions and increasing Ge content effectively promotes the elastic anisotropy of these alloys.

3.6 *Hardness of Ti–15Nb–xGe alloys*

As underlined by Tian *et al* [51], hardness can be described as the ability of a material's resistance to being scratched or dented by other material. Further, hardness of a material represents one of the common and fundamental mechanical properties of materials. Figure 8 depicts the Tian hardness (H_{Tian}) of Ti–15Nb–*x*Ge alloys for the considered composition range. Maximum hardness of these alloys emerges with 0.79 GPa for 0.8% Ge and decrease to minimum value of 0.13 GPa with increasing Ge concentration. Noteworthy to mention here that obtained hardness values of this study compares favourably the dentin hardness of human teeth with 0.25–0.80 GPa [52]. This result also implies that Ti–15Nb–*x*Ge alloys with compositions between Ge 0.8% and Ge 1.6% can be handy and safe for the applications of dental implants with also their low elastic moduli in the human body as pointed out above.

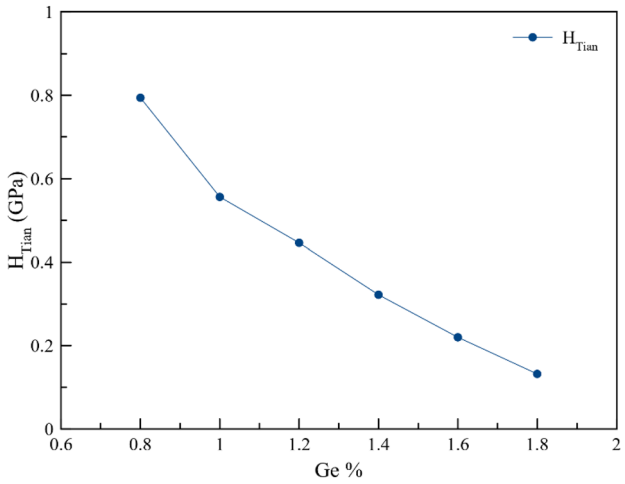

Figure 8. Hardness values of Ti–15Nb–*x*Ge alloys.

4. Conclusions

We can summarize the significant conclusions from this work as follows:

(1) We theoretically calculated the elastic and mechanical properties of Ti–15Nb–*x*Ge alloys for the first time with GGA of DFT by employing PBE formalism through VCA method.
(2) In general, present obtained results for the computed compositions of the alloys well collaborate with some expected and desired features of biomaterials, such as ductility and low Young's modulus.
(3) Small additions of Ge element (between 0.8 and 1.8%) to Ti–15Nb alloys definitely reduce the elastic and mechanical properties of the alloy. Therefore, this study can be further extended to other Ti–Nb alloys with higher Nb concentrations, i.e., Ti–20Nb, Ti–25Nb and Ti–30Nb within α-phase region of Ti–Nb alloys.
(4) Although this study was performed theoretically, some further experimental confirmations are still needed for the applications of Ti–15Nb–*x*Ge alloys as novel biomaterials either in the implantation zone of the orthopaedics or dentistry part of the medical sciences.
(5) Finally, we hope the results of this work, add value to existing literature and motivate both experimental and theoretical surveys in the near future to contribute in the application fields of biomaterials science and technology.

Acknowledgements

We gratefully acknowledge the help of Prof S H Naqib from the University of Rajshahi, Rajshahi, Bangladesh, for his careful reading of the paper.

References

[1] Zhang Y, Sun D, Cheng J, Tsoi J and Chen J 2019 *Regen. Biomater.* **7** 119
[2] Friák M, Counts W A, Ma D, Sander B, Holec D, Raabe D *et al* 2012 *Materials* **5** 1853
[3] Lei Z, Zhang H, Zhang E, You J, Ma X and Bai X 2020 *J. Biomater. Appl.* **34** 1368
[4] Han M K, Kim J Y, Hwang M J, Song H J and Park Y J 2015 *Materials* **8** 5986
[5] Marker C, Shang S L, Zhao J C and Liu Z K 2018 *Comput. Mater. Sci.* **142** 215
[6] Mishchenko O, Ovchynnykov O, Kapustian O and Pogorielov M 2020 *Materials* **13** 1306
[7] Li Q, Ma G, Li J, Niinomi M, Nakai M, Koizumi Y *et al* 2019 *J. Mater. Sci.* **54** 8675
[8] Guillem-Martí J, Herranz-Díez C, Shaffer J E, Gil F J and Manero J M 2015 *Mater. Sci. Eng. A* **636** 507
[9] Guo Y, Georgarakis K, Yokoyama Y and Yavari A R 2013 *J. Alloys Compd.* **571** 25
[10] Calin M, Helth A, Gutierrez Moreno J J, Bönisch M, Brackmann V, Giebeler L *et al* 2014 *Materials* **39** 162
[11] Zadorozhnyy V, Ketov S V, Wada T, Wurster S, Nayak V, Louzguine-Luzgin D V *et al* 2019 *Metals* **10** 34
[12] Miura K, Yamada N, Hanada S, Jung T K and Itoi E 2011 *Acta Biomater.* **7** 2320
[13] Niinomi M and Nakai M 2011 *Int. J. Biomater.* **2011** 1
[14] Stepanovska J, Matejka R, Rosina J, Bacakova L and Kolarova H 2020 *Biomed. Pap.* **164** 23
[15] Zhenhuan W, Yu D, Junsi L, Xiaowei J, Zongyu X, Li L *et al* 2020 *Biomed. Mater.* **15** 04517
[16] Liu X, Chen S, Tsoi J K H and Matinlinna J P 2017 *Regen. Biomater.* **4** 315
[17] Niinomi M, Liu Y, Nakai M, Liu H and Li H 2016 *Regen. Biomater.* **3** 173
[18] Kanchana V 2009 *EPL* **87** 26006
[19] Helth A, Pilz S, Kirsten T, Giebeler L, Freudenberger J, Calin M *et al* 2017 *J. Mech. Behav. Biomed.* **65** 137
[20] Meng Q, Guo S, Liu Q, Hu L and Zhao X 2014 *Prog. Nat. Sci.* **24** 157
[21] Xu W, Wu X, Stoica M, Calin M, Kühn U, Eckert J *et al* 2012 *Acta Mater.* **60** 5067
[22] Hao Y L, Li S J, Sun S Y, Zheng C Y and Yang R 2007 *Acta Biomater.* **3** 277
[23] Al-Zain Y, Kim H Y, Hosoda H, Nam T H and Miyazaki S 2010 *Acta Mater.* **58** 4212
[24] Kim H Y, Ikehara Y, Kim J I, Hosoda H and Miyazaki S 2006 *Acta Mater.* **54** 2419
[25] Li P, Ma X, Wang D and Zhang H 2019 *Metals* **9** 712
[26] Niranjan K R, Ameyama M K and Dey S R 2017 *Model. Simul. Mat. Sci. Eng.* **25** 85013
[27] Karre R, Niranjan M K and Dey S R 2015 *Mater. Sci. Eng. C* **50** 52
[28] Kim H S, Kim W Y and Lim S H 2006 *Scr. Mater.* **54** 887
[29] Zhang S-Z, Cui H, Li M-M, Yu H, Vitos L, Yang R *et al* 2016 *Mater. Des.* **110** 80
[30] Zhang D C, Mao Y F, Li Y L, Li J J, Yuan M and Lin J G 2013 *Mater. Sci. Eng. A* **559** 706
[31] Guo S, Shang Y, Zhang J, Meng Q, Cheng X and Zhao X 2017 *Intermetallics* **86** 20

[32] Masumoto K, Horiuchi Y, Inamura T, Hosoda H, Wakashima K, Kim H Y *et al* 2006 *Mater. Sci. Eng. A* **438–440** 835
[33] Jawed S F, Rabadia C D, Liu Y J, Wang L Q, Li Y H, Zhang X H *et al* 2019 *Mater. Des*. **181** 108064
[34] Clark S J, Segall M D, Pickard C J, Hasnip P J, Probert M I J, Refson K *et al* 2005 *Z. Kristallogr.* **220** 567
[35] Segall M D, Lindan P J D, Probert M J, Pickard C J, Hasnip P J, Clark S J *et al* 2002 *J. Phys. Condens. Matter* **14** 2717
[36] Perdew J P, Burke K and Ernzerhof M 1996 *Phys. Rev. Lett.* **77** 3865
[37] Perdew J P, Burke K and Ernzerhof M 1998 *Phys. Rev. Lett*. **80** 891
[38] Vanderbilt D 1990 *Phys. Rev. B* **41** 7892
[39] Monkhorst H J and Pack J D 1976 *Phys. Rev. B* **13** 5188
[40] Winkler B, Pickard C J and Milman C 2002 *Chem. Phys. Lett*. **362** 266
[41] Güler E and Güler M 2015 *Appl. Phys. A* **119** 721
[42] Ikehata H, Nagasako N, Furuta T, Fukumoto A, Miwa K and Saito T 2004 *Phys. Rev. B* **70** 174113
[43] Allard S 1969 *International tables of selected constants: thermal and mechanical data* (New York: Pergamon Press)
[44] Güler M and Güler E 2017 *Crystals* **7** 164
[45] Güler M and Güler E 2017 *Crystals* **7** 161
[46] Güler E and Güler M 2014 *Mater. Res*. **17** 1268
[47] Güler E and Güler M 2014 *Chin. J. Phys.* **52** 1625
[48] Güler M, Uğur Ş, Uğur G and Güler E 2020 *J. Mol. Struct.* **1200** 127150
[49] Pugh S F 1954 *Lond. Edinb. Dubl. Philos. Mag.* **45** 823
[50] Ranganathan S I and Ostoja-Starzewski M 2008 *Phys. Rev. Lett.* **101** 055504
[51] Tian Y, Xu B and Zhao Z 2012 *Int. J. Refract. Metals Hard. Mater*. **33** 93
[52] Chen P, Lin A, Lin Y, Seki Y, Stokes A, Peyras J *et al* 2008 *J. Mech. Behav. Biomed. Mater*. **1** 208